Med Biol Eng Comput (2010) 48:489–496
DOI 10.1007/s11517-010-0576-3

SHORT COMMUNICATION

A method to determine in vivo, specific airway compliance, in humans

Vanessa J. Kelly · Nathan J. Brown · Gregory G. King · Bruce R. Thompson

Received: 16 October 2009 / Accepted: 9 January 2010 / Published online: 9 March 2010

Abstract In order to understand the pathophysiology of diseases such as asthma and chronic obstructive pulmonary disease, it is essential to measure the mechanical properties of the airways. Currently, there are no methods to measure and quantify in vivo airway compliance in humans. In order to develop a method, we generated a curve-fitting algorithm that combines airway diameter measurements by high resolution computed tomography with pressure–volume curves obtained by the esophageal balloon technique. Our method allows the description of diameter–pressure curves for airways of varying size, presented as a 3D surface, from which specific airway compliance can be determined at any transpulmonary pressure. Applying this method to data from two healthy subjects, we found that small airways are more compliant than large airways and specific airway compliance was greatest at low transpulmonary pressures. In conclusion, our 3D surface is a useful tool to measure and quantify in vivo specific airway compliance in humans.

Keywords HRCT airway dimensions · Airway compliance · Pressure–diameter

List of symbols

D	Airway lumen diameter
FRC	Functional residual capacity
TLC	Total lung capacity
MID	Volume midway between TLC and FRC, FRC + (TLC − FRC)/2
P_{el}	Lung elastic pressure
V	Lung volume

Sub/superscripts

FRC	Measurements at FRC
MID	Measurements at the MID volume
TLC	Measurements at TLC
n	Normalized measurement
P–V	Pressure–volume

1 Introduction

In respiratory diseases such as asthma and chronic obstructive pulmonary disease (COPD), airflow limitation is one of the main correlates of symptom severity, morbidity, and mortality [18–20]. Airflow limitation occurs due to abnormal airway function, namely, reduced airway lumen area [24] and reduced airway compliance [1, 7, 31, 33]. Abnormal airway function may result from altered smooth

V. J. Kelly · B. R. Thompson
Department of Medicine, Nursing and Health Sciences, Monash University, Clayton, VIC, Australia

V. J. Kelly · N. J. Brown · G. G. King · B. R. Thompson
Co-operative Research Centre for Asthma and Airways, Glebe, NSW, Australia

V. J. Kelly · N. J. Brown · G. G. King
The Woolcock Institute of Medical Research, Glebe, NSW, Australia

V. J. Kelly · B. R. Thompson (✉)
The Department of Allergy, Immunology and Respiratory Medicine, The Alfred, Commercial Rd, Prahran, VIC, Australia
e-mail: B.Thompson@alfred.org.au

G. G. King
The Department of Respiratory Medicine, Royal North Shore Hospital, St Leonards, NSW, Australia

muscle dynamics [17], airway remodeling [25], and/or reduced parenchymal tethering on the airways [21]. As such, measurements of airway function, particularly airway compliance, are essential for understanding the pathophysiology and progression of obstructive lung diseases.

Airway compliance is defined as the change in airway dimensions that result from changes in transmural pressure. In vivo measurement of airway compliance in the form of airway diameter–pressure relationships have been made in animal models [2, 3, 6, 12]. Brown et al. [2, 3] demonstrated in dogs that airway compliance was decreased, or increased, in association with smooth muscle contraction, or relaxation, respectively. The curvilinear shape of the airway diameter–pressure relationship in these animal studies suggests that, rather than being a constant, airway compliance varies across the entire range of physiological transpulmonary pressures. The ability to quantify airway compliance at any transpulmonary pressure, i.e., instantaneous airway compliance, has the potential to provide additional insight into the physiological and clinical significance of airway mechanical properties.

In humans, direct measurement of airway compliance is difficult, and an indirect or surrogate measure of airway compliance, known as airway distensibility, has been developed [5, 7, 14, 31, 33]. Airway distensibility refers to the change in airway dimensions due to altered lung volume which is an important measurement in a number of diseases such as asthma. However, a limitation of the distensibility technique is that decreased airway distensibility may not be due to decreased airway compliance only, but also to increased lung compliance [8]. In patients with asthma, it was shown that airway distensibility, measured by the forced oscillation technique, was not related to lung elastic recoil [7]; however, it is not known whether the same is true for patients with COPD who have more extensive lung tissue abnormalities. In order to confidently attribute deficiencies in airway compliance to an airway abnormality rather than a lung tissue abnormality, it is necessary to measure changes in airway size with respect to changes in airway distending pressure [8]. However, there is currently no method to directly assess in vivo airway compliance in humans.

In this study, we used high resolution computed tomography (HRCT) measurements of airway diameter, and pressure–volume recordings to generate airway diameter–pressure relationships for airways of varying size, and presented them as a continuous 3D surface. This surface allows the determination of specific airway compliance at any transpulmonary pressure (instantaneous compliance) for airways of varied size. Our method is a novel tool that may elucidate more detailed information about changes in airway mechanics with diseases such as asthma and COPD.

2 Methods

2.1 Subjects

Subjects were recruited from advertisements at the Woolcock Institute of Medical Research (Sydney, Australia). Subjects were free of asthma and other respiratory or cardiac illnesses, current non-smokers with a less than ten pack year smoking history, and free of symptoms of acute respiratory infection. The study was approved by the Human Ethics Committee of The University of Sydney (Protocol No. X03-0222) and subjects gave written, informed consent.

2.2 Experimental design

The subjects were tested on three separate days. During visit one, subjects completed spirometry and lung volume testing. The second visit included spirometry and partial HRCT scans while breathing on a pneumotach. HRCT scans were obtained during a voluntary breath-hold of approximately 15 s at the lung volumes FRC, TLC, and a volume approximately 50% between FRC and TLC (MID), referred to as V_{FRC}, V_{TLC}, and V_{MID}, respectively. Subjects were instructed to breath-hold at the appropriate lung volume by a trained scientist who had visual feedback via a real-time spirogram. Breath-holds were rehearsed prior to the scan. Subjects inhaled maximally to TLC and breath-held during the TLC scan. Scans at MID were obtained by inhalation to TLC then exhaling to a predetermined volume and scans at FRC through a breath-hold at end expiration from a normal tidal breath. Breath-holds were followed by maximal inhalation to TLC to allow verification of the lung volume at which they were scanned. On the third visit subjects completed esophageal pressure–volume measurements.

2.3 Equipment and measurements

Spirometry was performed using a Vmax 20c spirometer (Sensormedics Corporation Yorba Linda, CA, USA) and a Spiropro® hand-held spirometer (Viasys Healthcare GmbH, Hoechberg, Germany) during visit one and two, respectively. Lung volumes were measured using an Autobox 6200 DL plethysmograph (Sensormedics Corporation, Yorba Linda, CA, USA). Spirometry and lung volumes were performed to meet the ATS/ERS acceptability and repeatability criteria [23, 30]. Predicted values described by NHANES III [13] and Crapo [10] were used for spirometry and lung volumes, respectively.

HRCT scanning was completed using a Sensation 16 slice CT Scanner (Siemens AG Berlin, Germany), using settings of 120 kVp and 100 mAs with a slice thickness of 1.0 mm and a rotation of 0.75 s with a table speed of 13 mm s^{-1}. HRCT images were reconstructed using a high

spatial frequency algorithm and a 30-cm field of view to a 512 × 512 matrix yielding a voxel dimension of 0.58 × 0.58 × 1.0 mm. Esophageal pressure–volume (P–V) curves were measured according to the method described by Brown et al. [7], where a 10-cm long thin latex balloon was swallowed to predetermined depth [9], filled with 0.5 ml of air, and transpulmonary pressure measured during a deflation maneuver. Individual P–V curves for each subject were characterized by the expression $V = x - ye^{-zP}$ [9] using MATLAB (The Mathworks, Natick, MA, USA). The P–V curves were determined from the change in pressure (P_{el}) from FRC and lung volume represented as %TLC. Individual curve fits for each subject were generated, and the mean P–V curve determined by averaging the coefficients of the individual P–V curves.

2.4 HRCT image analysis

On each HRCT scan, airway segments were identified and matched across several digital image (DICOM format) slices, between scans, and at different lung volumes, using airway bifurcations as anatomical landmarks. An airway segment was defined as a section of airway lying between two consecutive airway branch points.

On each image, mean lumen area was measured using a semi-automated analysis program (WinImageBase, version 1.8.3), which has been previously validated against excised lung as a calibration standard [11]. In brief, airway cross sections were identified on each HRCT image. Radial vectors extending from the centroid to the boundary of the region of interest were generated at equal angles (Fig. 1a). Each radial vector was analyzed to determine the points at which the greatest change in pixel intensity occurred, defining the air–tissue barrier. Airway lumen area was calculated from the number of pixels within the lumen perimeter, and averaged across each slice. Since airway size is commonly described by diameter [2, 16, 27], mean airway lumen cross-sectional area was translated to idealized airway diameter, assuming a circular lumen [11]. No corrections were made for the airway angle.

2.5 Determination of airway compliance surface

Airway lumen diameters (D) were measured from HRCT at three lung volumes, FRC (D_{FRC}), MID (D_{MID}), and TLC (D_{TLC}), during deflation. The change in diameter with lung volume was assessed for significance through comparisons of the D_{FRC}, D_{MID}, and D_{TLC} data sets. In order to enable comparison between airways of different sizes, measurements of D_{FRC}, D_{MID}, and D_{TLC}, for each airway, were normalized (n) to their corresponding D_{FRC} measurement and referred to as $D_{n_{FRC}}$, $D_{n_{MID}}$, and $D_{n_{TLC}}$ [29], such that $D_{n_{FRC}}$ therefore equals 1. $D_{n_{MID}}$ and $D_{n_{TLC}}$ data points for both subjects at each lung volume were then grouped and plotted together against absolute diameter D_{FRC}. Subsequently, nonlinear regression was performed on the data using the exponential expression $y = a + be^{-kx}$ to determine two relationships: (1) the increase in diameter from FRC to MID with respect to diameter at FRC, $D_{n_{MID}}(D_{FRC})$, and (2) the increase in diameter from FRC to TLC with respect to the diameter at FRC, $D_{n_{TLC}}(D_{FRC})$ (Fig. 1b). The exponent k was determined from the $D_{n_{TLC}}(D_{FRC})$ relationship, where the greatest degree of expansion occurred, and was maintained throughout the subsequent regressions. Notably, the $D_{n_{MID}}(D_{FRC})$ regression using the fixed exponent did not exhibit a significant loss of strength (Fisher Z test, $p = 0.34$). The difference between regression curves for $D_{n_{MID}}(D_{FRC})$ and $D_{n_{TLC}}(D_{FRC})$ was assessed based on differences between the coefficients a and b.

In order to generate a 3D representation of specific airway compliance, where compliance is described as specific because the change in airway diameter is represented as normalized change, airway diameter measurements were combined with the mean P–V curve. In particular, this involved three steps. First, the change in P_{el} associated with the absolute change in diameter that occurred between each volume (V_{FRC}, V_{MID}, V_{TLC}) was determined by translating the breath-hold volumes during the HRCT scans (V_{FRC}, V_{MID}, and V_{TLC}) to the corresponding change in lung elastic pressure from FRC (P_{FRC}, P_{MID}, and P_{TLC}) using the mean P–V curve (Fig. 1c). Based on the assumption that airway pressure is equal to lung elastic pressure [28], the lung elastic pressures (P_{FRC}, P_{MID}, and P_{TLC}) were used to distribute the $D_{n_{FRC}}(D_{FRC})$, $D_{n_{MID}}(D_{FRC})$, and $D_{n_{TLC}}(D_{FRC})$ regression curves on a third axis of P_{el} (Fig. 1d). Second, in order to determine pressure–diameter relationships, $D_n(P_{el})$, for airways of each diameter (D_{FRC}), curve fitting was employed to interpolate between the three values of $D_n(P_{el})$ for each airway size

Fig. 1 The four step process to generate specific airway compliance. ▶ **a** HRCT identified airway, spiral vectors determine airway lumen edge and subsequently calculate lumen diameter. **b** Exponential regression results for the normalized change in diameter (D_n) at V_{FRC} (*solid line*), V_{MID} (*dotted line*) and V_{TLC} (*dashed line*), $D_{n_{FRC}}(D_{FRC})$, $D_{n_{MID}}(D_{FRC})$ and $D_{n_{TLC}}(D_{FRC})$, respectively. **c** Mean pressure–volume (P–V) regression curve ($V = 103.76 - 55.53e^{-0.1261P}$) generated from subject 1 (*open squares*) and subject 2 (*open circles*) data. HRCT volume measurements V_{FRC} (*solid line*), V_{MID} (*dotted line*), and V_{TLC} (*dashed line*) translated to change in lung elastic pressures (P_{el}) P_{FRC}, P_{MID}, and P_{TLC}. **d** Regression results $D_{n_{FRC}}(D_{FRC})$, $D_{n_{MID}}(D_{FRC})$ and $D_{n_{TLC}}(D_{FRC})$, placed along the third P_{el} axis at P_{FRC}, P_{MID}, and P_{TLC}. **e** Iterative curve fitting between $D_{n_{FRC}}(D_{FRC})$, $D_{n_{MID}}(D_{FRC})$, and $D_{n_{TLC}}(D_{FRC})$ along the P_{el} axis allows the relationship $D_n(P_{el})$ to be described continuously. **f** Iterative curve fitting from 1e allows the A and K coefficients to be described with respect to D_{FRC} for a complete description of airway compliance with respect to pressure and airway size, $D_n(D_{FRC}, P_{el})$. Note that the x-axis in **b** and **f** are reversed for consistency with **d** and **e**

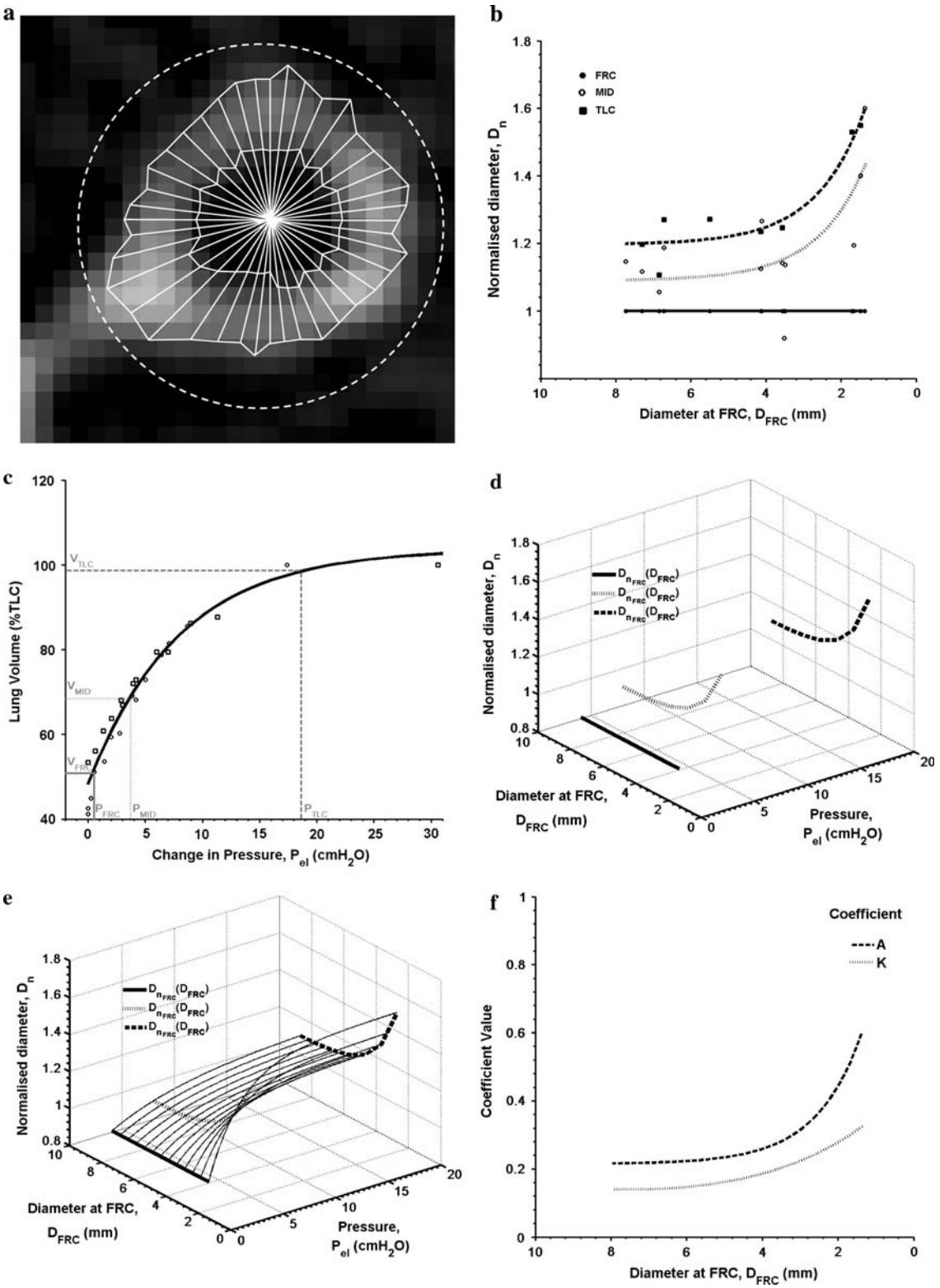

using the expression $1 + A\left(1 - e^{(KP_{el})}\right)$, based on Colebatch [9] (Fig. 1e). This process effectively generated a pressure–diameter curve, with coefficient values A and K, for each airway size (Fig. 1f). In order to develop a continuous description of the specific compliance of airway diameter with respect to D_{FRC} and P_{el}, $D_n(D_{FRC}, P_{el})$, changes in A and K with respect to D_{FRC} were described continuously using exponential equations sufficient to

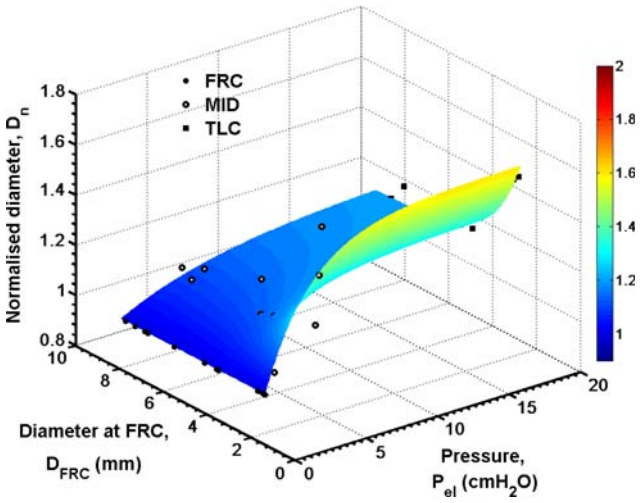

Fig. 2 Airway compliance with respect to pressure (P_{el}) and airway size (D_{FRC}), $D_n(D_{FRC}, P_{el})$. This surface shows small airways undergo a larger fractional increase in diameter (D_n) with increasing pressure than larger airways. The contour of the surface represents specific airway compliance with changing pressure. A steep contour indicates high compliance, and a gentle contour a low compliance

achieve $R^2 > 0.9999$ (Table 2). Finally, a complete set of expressions for the description of specific airway compliance is given by;

$$D_n(D_{FRC}, P_{el}) = 1 + A(D_{FRC})\left(1 - e^{(-K(D_{FRC})P_{el})}\right) \quad (1)$$

where $A(D_{FRC})$ and $K(D_{FRC})$ describe the change of the coefficients for the pressure–diameter curves $D_n(P_{el})$ for varying airway size. The final 3D representation (Fig. 2) reflects diameter–pressure curves for each airway size, plotted together, where the gradient of the surface with respect to P_{el} represents the compliance.

The relationships, $A(D_{FRC})$ and $K(D_{FRC})$, characterize the features of the diameter–pressure curves at each airway diameter. $A(D_{FRC})$ represents the maximum degree of expansion from the initial value. $K(D_{FRC})$ describes the curvature, whereby a larger value equates to a smaller pressure required to increase D_n from the initial value to the asymptote $(1 + A(D_{FRC}))$. The plateau pressure, P_p, defined as the pressure at which 95% of the expansion of the airway has occurred can be determined from, $P_p = 3/K(D_{FRC})$ (Fig. 3a). Finally, the derivative of the $D_n(D_{FRC}, P_{el})$ relationship (Eq. 1) allows specific airway compliance (C_n) to be described for any airway size at any P_{el} (Eq. 2).

$$C_n(D_{FRC}, P_{el}) = K(D_{FRC})A(D_{FRC})e^{(-K(D_{FRC})P_{el})} \quad (2)$$

2.6 Statistical analysis

Data are shown as means with standard errors unless otherwise stated. In order to assess the change in diameter between V_{FRC}, V_{MID}, and V_{TLC}, one way RM ANOVA with Student–Newman–Keuls post-hoc analysis were performed on consecutive data sets D_{FRC}, D_{MID}, and D_{TLC}. The T statistic was used to assess differences between the individual P–V curve fits and between the coefficients of the curve fits for $D_{FRC}(D_{n_{FRC}})$, $D_{FRC}(D_{n_{MID}})$, and $D_{FRC}(D_{n_{TLC}})$.

3 Results

Two male subjects took part in the study. Subject demographics and lung function results, which were within normal limits, appear in Table 1. From the HRCT scans, 22 individual airway segments were identified from the intermediate and lower lobe bronchi. Airways identified at only one lung volume or not identified at FRC were

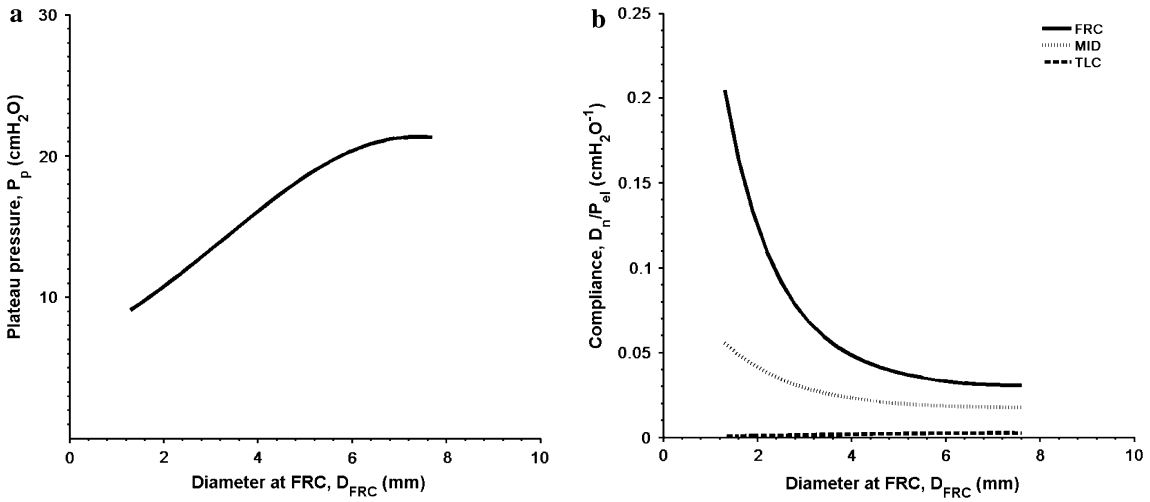

Fig. 3 Plateau pressure (P_p) and compliance (C_n) at P_{FRC}, P_{MID}, and P_{TLC} determined from 3D compliance surface. P_p is proportional to airway size (**a**). Compliance at P_{FRC} and P_{MID} are inversely proportional to airway size and greater than the compliance at P_{TLC}, respectively

Table 1 Anthropometric characteristics and lung function results for Subject 1 and 2

	Units	Subject 1	Subject 2
Age	year	23	29
Height	cm	181.0	174.5
Weight	kg	97.5	70.5
TLC	% predicted (L)	100.9	84.2
FRC	% predicted (L)	87.6	79.5
RV	% predicted (L)	93.8	83.7
RV/TLC	%	21.2	23.0
FEV_1	% predicted (L s^{-1})	102.3 (4.9)	84.1 (3.6)
FVC	% predicted(L s^{-1})	106.1 (6.2)	82.6 (4.2)
FEV_1/FVC	%	79.6	83.5

excluded, leaving 14 airways (Subject 1: 3 airways; Subject 2: 11 airways) included in the analysis ranging from 1.4 to 7.7 mm. The breath-hold volumes during the HRCT scans were averaged, due to similarity of the lung volumes, with the following results, V_{FRC} (51.6% TLC), V_{MID} (75.9% TLC), and V_{TLC} (99.6% TLC). P_{FRC} (0 cm H_2O), P_{MID} (3.96 cm H_2O), and P_{TLC} (17.92 cm H_2O) were calculated using the mean P–V curve (Fig. 1c).

3.1 Specific airway compliance

Airway diameters at V_{MID} (mean $D_{n_{MID}} = 1.20 \pm 0.05$) and V_{TLC} (mean $D_{n_{TLC}}$ 1.30 ± 0.06) were significantly greater than at V_{FRC} ($p < 0.001$), however, the difference between MID and TLC did not reach significance ($p = 0.09$). Normalized diameter data for $D_{n_{FRC}}(D_{FRC})$, $D_{n_{MID}}(D_{FRC})$, and $D_{n_{TLC}}(D_{FRC})$ are shown in Fig. 1b. $D_{n_{TLC}}$ was greater in the smaller sized airways compared to the larger sized airways, which demonstrates that specific compliance increases with decreasing airway size. The equation coefficients, R^2 and p values for these regressions are included in Table 2. Each Regression was statistically significant ($p < 0.05$). Comparison of the coefficients between $D_{n_{MID}}(D_{FRC})$ and $D_{n_{TLC}}(D_{FRC})$ showed no significant differences in a ($p = 0.09$) or b ($p = 0.76$).

The normalized change in diameter (D_n) as a function of airway diameter at FRC (D_{FRC}) and pressure (P_{el}), referred to as $D_n(D_{FRC}, P_{el})$, is presented continuously as a 3D surface (Fig. 2) which quantifies how the pressure–diameter curve changes with airway size. Changes in the shape of the pressure–diameter curve are characterized by the coefficient relationships $A(D_{FRC})$ and $K(D_{FRC})$, which fall progressively with increasing airway diameter (Fig. 1f). Based on these coefficients, we observed that airway plateau pressure P_p increases progressively with increasing airway diameter. We found that P_p is greater for larger airways and lower in smaller airways (Fig. 3a). Calculation of the instantaneous compliance at P_{FRC}, P_{MID}, and P_{TLC}, showed greater compliance at P_{FRC} compared to P_{MID} and P_{TLC}, and that compliance at P_{FRC} and P_{MID} was inversely related to airway size (Fig. 3b).

4 Discussion

This study describes a novel method to determine in vivo airway diameter–pressure curves for airways of varying size in humans. In addition, the method allows specific compliance to be determined at any transpulmonary pressure for a range of different sized airways. The method incorporates HRCT measurements of airway diameter with pressure–volume recordings to generate a unique description of specific airway compliance over a range of distending pressures. We found that smaller airways expand to a greater extent than larger airways, consistent with previous studies in animals [1, 29]. In addition, specific airway compliance is greatest at low pressures (FRC) and decreases with increasing airway size. This corresponded to airway plateau pressure increasing progressively with airway size.

Several methodological issues warrant discussion, which include assumptions used, technical limitations, and sample size. The assumptions of the study were: (1) That data obtained from both subjects were comparable and therefore grouping these data was appropriate. This was considered reasonable as subject anthropometrics were similar and, at the lung volumes measured during HRCT scans, individual P–V regressions were also similar; (2) That the gravitational effect on pleural pressure was

Table 2 Regression coefficients for $D_{n_{TLC}}(D_{FRC})$ and $D_{n_{MID}}(D_{FRC})$ along with regression equations for the continuous description of $A(D_{FRC})$ and $K(D_{FRC})$

Value (mean ± s.e.)	a	b	k	R^2	p
$D_{n_{TLC}}(D_{FRC})$	1.197 ± 0.039	1.159 ± 0.474	0.776 ± 0.309	0.893	0.004
$D_{n_{MID}}(D_{FRC})$	1.090 ± 0.045	0.986 ± 0.278	0.776	0.556	0.005
$A(D_{FRC})$	$0.215 + 1.196e^{(-0.826D_{FRC})}$				
$K(D_{FRC})$	$0.432e^{(-0.297D_{FRC})} + 0.0230e^{(0.152D_{FRC})}$				

Equation form: $D_n(D_{FRC}) = a + be^{-kD_{FRC}}$

negligible, and therefore corrections for variations in pleural pressure with gravity [22] were not included; (3) That changes in the esophageal pressure corresponded to changes in the airway transmural pressure, which is valid during breath-hold maneuvers [28], such as those completed during the HRCT scanning. In the presence of parenchymal uncoupling [21] this assumption may be invalid, although unlikely in this study due to the use of normal healthy subjects, in whom lung tissue abnormalities would not be expected. The potential effect of a loss of airway-parenchymal tethering in disease would be reduced airway distension during lung inflation. Therefore, airways would appear less compliant, if measured using the current method; yet it would be unclear whether this was due to airway stiffening or impaired transmission of airway distending forces. This will remain an issue until better methods of measuring airway-parenchymal tethering are developed.

Technical limitations include: (1) The postural mismatch between volume and pressure measurements. Lung volume [32], lung compliance, and P_{FRC} [32] will be reduced in the supine position, during HRCT scans, compared to the upright position. This is a common issue in HRCT studies and we have attempted to minimize its impact, by measuring relative lung volume changes, from maximal lung inflation, during the supine HRCT scans. Maximal lung inflation, measured during HRCT, was matched to TLC, which was measured in the upright position. However, the important measurement is the relative change in lung volume during the scan, which was measured supine. The reduction in lung compliance in the supine position is not accounted for in this study, but the likely effect would be an overall reduction in airway compliance. (2) It has been reported that HRCT measurements of airway lumen area are underestimated in small airways [4, 34], which would result in an overestimation of compliance. However, the magnitude of effect between different airway sizes is difficult to estimate. Importantly, in this study, we used a lumen measurement method [11, 15] where although precision is reduced in the smaller airways, we validated the method to be specifically bias free, avoiding potential errors in calculated compliance.

The sample size of the study and hence the power of the 3D surface could be improved by the addition of more airway measurements by either increasing the number of subjects in the study or making airway dimension recordings at a fourth or fifth lung volume. However, the small sample size was sufficient to demonstrate the functionality of the method while minimizing radiation exposure to the subjects.

Despite the limitations of the study, the foundation of the surface was a statistically strong set of regression curves. More importantly, the method enables a description of specific airway compliance to be developed from in vivo, human data, which has not previously been possible.

The 3D surface model generated in this study suggests that airways do not dilate isotropically with lung inflation. The airway diameter–pressure curves vary with airway size, which would not have occurred with isotropic lung expansion. This finding is in agreement with similar work in dogs [2]. Based on our 3D surface model, our study found for the first time in adult humans that small airways are more compliant than large airways which is in agreement with prior studies in mice [29] and have lower plateau pressures than larger airways. The mechanism for the increased specific compliance of small airways is likely due to differences in airway wall composition, specifically decreased or absent cartilage in small airways compared with large airways [26]. The greater specific compliance and lower plateau pressure in the smaller airways may also be of major importance for minimizing airflow resistance during breathing.

In conclusion, we have described a new method for determining in vivo airway diameter–pressure relationships in humans, in a manner which allows quantification of specific airway compliance for any transpulmonary pressure across a range of airway sizes. The measurement of specific airway compliance has many potential applications in studies of airflow limitation. It will allow realistic in vivo airway compliance values for mathematical assessment of airflow resistance during breathing to be determined. It has the potential to examine, in detail, changes in airway mechanics during the transition from mild disease to chronic and life threatening airflow limitation, which is still poorly understood.

Acknowledgment This work was supported by the Co-operative Research Council for Asthma and Airways, NHMRC Project Grant 512387, NHMRC Scholarship 521808 and The Neil and Norma Hill Asthma Foundation of NSW Grant.

References

1. Brackel HJ, Pedersen OF, Mulder GH et al (2000) Central airways behave more stiffly during forced expiration in patients with asthma. Am J Respir Crit Care Med 162:896–904
2. Brown RH, Mitzner W (1996) Effect of lung inflation and airway muscle tone on airway diameter in vivo. J Appl Physiol 80:1581–1588
3. Brown RH, Mitzner W, Bulut Y et al (1997) Effect of lung inflation in vivo on airways with smooth muscle tone or edema. J Appl Physiol 82:491–499
4. Brown RH, Georgakopoulos J, Mitzner W (1998) Individual canine airways responsiveness to aerosol histamine and methacholine in vivo. Am J Respir Crit Care Med 157:491–497
5. Brown RH, Scichilone N, Mudge B et al (2001) High-Resolution Computed Tomographic evaluation of airway distensibility and the effects of lung inflation on airway caliber in healthy subjects and individuals with asthma. Am J Respir Crit Care Med 163:994–1001
6. Brown RH, Mitzner W, Wagner E et al (2003) Airway distension with lung inflation measured by HRCT. Acad Radiol 10:1097–1103

7. Brown NJ, Salome CM, Berend N et al (2007) Airway distensibility in adults with asthma and healthy adults measured by the forced oscillation technique. Am J Respir Crit Care Med 176:129–137
8. Colebatch HJ, Finucane KE, Smith MM (1973) Pulmonary conductance and elastic recoil relationships in asthma and emphysema. J Appl Physiol 34:143–153
9. Colebatch HJ, Greaves IA, Ng CK (1979) Exponential analysis of elastic recoil and aging in healthy males and females. J Appl Physiol 47:683–691
10. Crapo R, Morris A, Clayton P et al (1982) Lung volumes in healthy non-smoking adults. Bull Eur Physiopathol Respir 18:419–425
11. Dame Carroll JR, Chandra A, Jones AS et al (2006) Airway dimensions measured from micro-computed tomography and high-resolution computed tomography. Eur Respir J 28:712–720
12. Hahn HL, Graf PD, Nadel JA (1976) Effect of vagal tone on airway diameters and on lung volume in anesthetized dogs. J Appl Physiol 41:581–589
13. Hankinson JL, Odencrantz JR, Fedan KB (1999) Spirometric reference values from a sample of the general U.S. population. Am J Respir Crit Care Med 159:179–187
14. Johns DP, Wilson J, Harding R et al (2000) Airway distensibility in healthy and asthmatic subjects: effect of lung volume history. J Appl Physiol 88:1413–1420
15. King GG, Muller NL, Whittall KP et al (2000) An analysis algorithm for measuring airway lumen and wall areas from high-resolution computed tomographic data. Am J Respir Crit Care Med 161:574–580
16. King GG, Carroll JD, Muller NL et al (2004) Heterogeneity of narrowing in normal and asthmatic airways measured by HRCT. Eur Respir J 24:211–218
17. Krishnan R, Trepat X, Nguyen TTB et al (2008) Airway smooth muscle and bronchospasm: fluctuating, fluidizing, freezing. Respir Physiol Neurobiol 163:17–24
18. Lange P, Parner J, Vestbo J et al (1998) A 15-year follow-up study of ventilatory function in adults with asthma. N Engl J Med 339:1194–1203
19. Mannino DM, Buist AS, Petty TL et al (2003) Lung function and mortality in the United States: data from the first national Health and Nutrition Examination Survey follow up study. Thorax 58:388–393
20. Mannino DM, Ford ES, Redd SC (2003) Obstructive and restrictive lung disease and functional limitation: data from the Third National Health and Nutrition Examination. J Inter Med 254:540–547
21. Mauad T, Silva LF, Santos MA et al (2004) Abnormal alveolar attachments with decreased elastic fiber content in distal lung in fatal asthma. Am J Respir Crit Care Med 170:857–862
22. Milic-Emili J, Henderson JA, Dolovich MB et al (1966) Regional distribution of inspired gas in the lung. J Appl Physiol 21:749–759
23. Miller MR, Hankinson J, Brusasco V et al (2005) Standardisation of spirometry. Eur Respir J 26:319–338
24. Nakano Y, Muller NL, King GG et al (2002) Quantitative assessment of airway remodeling using high-resolution CT. Chest 122:271S–275S
25. Niimi A, Matsumoto H, Amitani R et al (2000) Airway wall thickness in asthma assessed by computed tomography. Am J Respir Crit Care Med 162:1518–1523
26. Noble PB, Turner DJ, Mitchell HW (2002) Relationship of airway narrowing, compliance, and cartilage in isolated bronchial segments. J Appl Physiol 92:1119–1124
27. Okazawa M, Bai TR, Wiggs BR, Pare PD (1993) Airway smooth muscle shortening in excised canine lung lobes. J Appl Physiol 74:1613–1621
28. Otis AB, Proctor DF (1948) Measurement of alveolar pressure in human subjects. Am J Physiol 152:106–112
29. Sera T, Uesugi K, Himeno R et al (2007) Small airway changes in healthy and ovalbumin-treated mice during quasi-static lung inflation. Respir Physiol Neurobiol 156:304–311
30. Wanger J, Clausen JL, Coates A et al (2005) Standardisation of the measurement of lung volumes. Eur Respir J 26:511–522
31. Ward C, Johns DP, Bish R et al (2001) Reduced airway distensibility, fixed airflow limitation, and airway wall remodeling in asthma. Am J Respir Crit Care Med 164:1718–1721
32. Washko GR, O'Donnell CR, Loring SH (2006) Volume-related and volume-independent effects of posture on esophageal and transpulmonary pressures in healthy subjects. J Appl Physiol 100:8–753
33. Wilson J, Li X, Pain MC (1993) The lack of distensibility of asthmatic airways. Am Rev Respir Dis 148:806–809
34. Wood SA, Zerhouni EA, Hoford JD et al (1995) Measurement of three-dimensional lung tree structures by using computed tomography. J Appl Physiol 79:1687–1697